ELSEVIER

Surface Science 419 (1999) 79–88

surface science

Oxidation of Pt(111) by ozone (O_3) under UHV conditions

N.A. Saliba, Y.-L. Tsai, C. Panja, B.E. Koel *

Department of Chemistry, University of Southern California, Los Angeles, CA 90089-0482, USA

Received 6 April 1998; accepted for publication 12 August 1998

Abstract

Ozone (O_3) is a reactive oxidant, creating high effective oxygen pressures under ultra-high vacuum (UHV) conditions. Large oxygen concentrations up to $\Theta_O = 2.4$ ML were produced by ozone exposure on Pt(111) at 300 K and analyzed using temperature-programmed desorption (TPD), Auger electron spectroscopy (AES), and low-energy electron diffraction (LEED). O_2 desorption occurs in broad TPD peaks that shift from 814 to 558 K as the oxygen coverage increases from 0.03 to 0.95 ML. For coverages of $\Theta_O \geq 1.2$ ML, "undercutting" of the desorption curves occurs, along with a narrowing and shift to higher temperature, such that O_2 desorption occurs in a sharp (23 K wide) peak at 708 K at $\Theta_O = 2.4$ ML. LEED shows a (2×2) pattern for Θ_O near 0.25 ML, but then only a (1×1) pattern between 0.3 and 1.2 ML. For oxygen coverages larger than 1.2 ML, the Pt(111) surface is disordered. Using the leading edge method, we estimate that the desorption activation energy decreases from 45 to 20 kcal mol^{-1} with increased oxygen concentration for $0 < \Theta_O < 1.2$ ML, and thereafter increases with increasing concentration to 38 kcal mol^{-1} at $\Theta_O = 2.4$ ML. We interpret the O_2 desorption curves for $\Theta_O > 1.2$ ML as arising from decomposition of particles of platinum oxide of increasing size near the surface. A very weakly bound state of oxygen also exists at high Θ_O and desorbs at 390 K. Oxidized platinum is reduced upon heating to Pt metal in the temperature range of 674–708 K in UHV.

Keywords: Auger electron spectroscopy; LEED; Low index single crystal surfaces; Ozone; Pt(111) oxidation; Thermal desorption

1. Introduction

Pt catalyzes several important heterogeneous oxidation reactions, such as the oxidation of CO in automotive catalytic converters [1] and the oxidation of NH_3 in nitric acid synthesis [2], and so the adsorption of oxygen on Pt surfaces has been investigated extensively. For example, O_2/Pt(111) has been the subject of a number of studies [3–10]. Nonetheless, studies of the chemical state and reactivity of high concentrations of oxygen on Pt(111) under the controlled conditions of UHV have been limited previously by the relatively low coverage of adsorbed oxygen adatoms obtainable from O_2 dissociation under UHV conditions.

Oxygen adsorbs molecularly on Pt(111) at temperatures below 170 K and dissociates into oxygen adatoms at higher temperatures [4,7]. Chemisorbed oxygen adatoms obtained either by a saturation exposure of O_2 on Pt(111) at 300 K in UHV or by warming a saturation coverage of O_2(a) on Pt(111) to 300 K have a saturation coverage of 0.25 ML [8] on the Pt(111) surface, as referenced to the Pt(111) surface atom density (1.5×10^{15} atoms cm^{-2}). This surface gives a (2×2) LEED pattern [8]. Higher coverages of O adatoms on Pt(111) from O_2 exposures have been previously obtained in UHV by employing

* Corresponding author. Fax: +1 213 740 3972; e-mail: koel@chem1.usc.edu

0039-6028/99/$ – see front matter
PII: S0039-6028(98)00667-0

extraordinary methods. Gland [3] produced $\Theta_O = 0.53$ ML with extended temperature cycling, Steininger et al. [7] showed saturation oxygen coverages enhanced by a factor of two by using electron bombardment of molecular oxygen, Koel and coworkers [11,12] formed a maximum coverage of $\Theta_O = 0.75$ ML by the reaction of NO_2 with Pt(111) at 400 K, and Niehus et al. [9] reported an oxygen coverage near unity on Pt(111) after continuous exposures of the crystal at 540 K to 3×10^{-7} Torr of O_2.

Anodic oxide films have long been prepared by electrochemical oxidation of platinum in aqueous solution [13]. This oxidation is generally believed to occur by a two-step mechanism involving the rapid reversible adsorption of OH followed by a slower irreversible place-exchange process during which the platinum atoms and ions at the surface exchange places with oxygen containing species to form PtO_x films [13,14]. Measurements of multilayer surface oxidation of polycrystalline platinum at moderate oxygen pressures reveal that these platinum oxide films undergo rapid dissociation in 1 atm of air at 600–650°C (873–923 K) [15] with a heat of decomposition of (for either PtO_2 [15] or PtO [16]) of 42 kcal mol^{-1}. These results are consistent with thermal stabilities reported for a number of studies of oxidized Pt particles [15–22].

In this paper, we report using ozone, O_3, to generate high oxygen concentrations on Pt(111) and to form platinum oxide under UHV conditions. Ozone is a more reactive oxidant than NO_2 and has a very weak O–O bond with $D(O_2\text{–}O) = 25.5$ kcal mol^{-1} [23]. This extends our previous work on O_3/Au(111) [24]. The results of ozone exposures on Pt(100) [25], Sn/Pt(111) [26] and Sn/Pt(100) surface alloys [27] will be reported elsewhere.

2. Experimental

These experiments were performed in a two-level UHV chamber [28], with a base pressure of 2×10^{-10} Torr, pumped by a 220 l s^{-1} ion pump, a 170 l s^{-1} turbo molecular pump and a titanium sublimation pump. The chamber was equipped with a UTI 100C quadrupole mass spectrometer (QMS) for TPD, a double-pass cylindrical mirror analyzer (CMA) for AES and four-grid optics for LEED.

The Pt(111) (Atomergic, 5 N purity, 1 cm diameter) single crystal was cleaned using Ar^+ ion sputtering and O_2 treatment at 800–1000 K followed by annealing in a vacuum at 1200 K. The crystal was heated resistively via a pair of Ta wires in close contact with a liquid nitrogen reservoir. Sample temperatures of 90–1200 K were routinely achieved as measured by a chromel–alumel thermocouple that was spot-welded to the crystal edge. The substrate cleanliness was checked by AES prior to each gas exposure.

High-purity ozone was dosed onto the Pt(111) substrate via a glass microcapillary array doser. The synthesis and purification of ozone have been reported elsewhere [24]. Extensive passivation of the stainless-steel gas handling line and doser tube was necessary for reproducible ozone exposures. All O_3 exposures were carried out at a substrate temperature of 300 K in order to avoid the coadsorption of water. In addition, picking an exposure temperature and using roughly this value is important because the saturation oxygen coverage depends on the exposure temperature. Exposure values are given in units of Langmuirs (L) as determined by the background gas pressure in the chamber during dosing without any further corrections.

TPD spectra were taken using a linear heating rate of 4 K s^{-1} with the crystal in line-of-sight of the QMS ionizer. A stainless-steel shield with an entrance aperture diameter of 1 cm covered the ionizer region of the QMS. The crystal was placed at a distance of 1 mm in front of the aperture for TPD experiments, and this effectively attenuated background contributions to the TPD curves. In order to stop the electron emission from the QMS ionizer impinging on the substrate during TPD measurements, two pieces of highly transparent stainless steel screens were used–one across the end of the ionizer grid (with a bias of -55 V) and the other across the shield aperture (at ground potential).

AES measurements were taken at an incident beam energy of 3 keV using a beam current of

10 μA. No change in the O/Pt ratio was detected during the time frame of the AES measurements.

3. Results

O_2 (32 amu) TPD spectra following various exposures of ozone on Pt(111) at 300 K are shown in Figs. 1 and 2. Fig. 1 shows results after relatively low O_3 exposures, 0.1–1 L, which produced surface oxygen coverages of 0.03–0.95 ML. The determination of the oxygen coverage was made by comparison of the O_2 TPD peak areas in Figs. 1 and 2 to that from a saturation coverage of O_2 exposed on Pt(111) at 100 K and heated to room temperature to give $\Theta_O = 0.25$ ML [3]. At a small coverage of $\Theta_O = 0.03$ ML, Fig. 1 shows that O_2 desorbed in a peak at 814 K. This peak shifted to lower

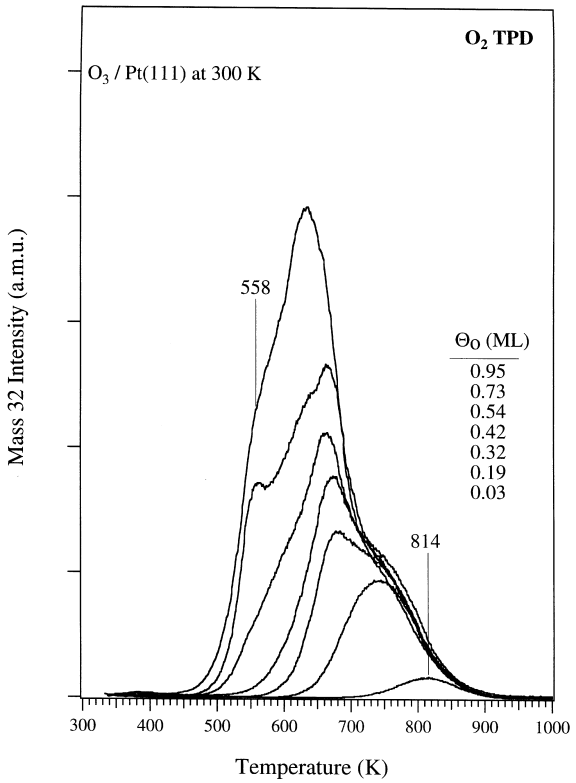

Fig. 1. O_2 TPD curves after O_3 exposures of 0.1–1 L on Pt(111) at 300 K. The coverages denoted as Θ_O were calibrated by using the O_2 TPD area following saturation exposures of O_2 to be $\Theta_O = 0.25$ ML [3].

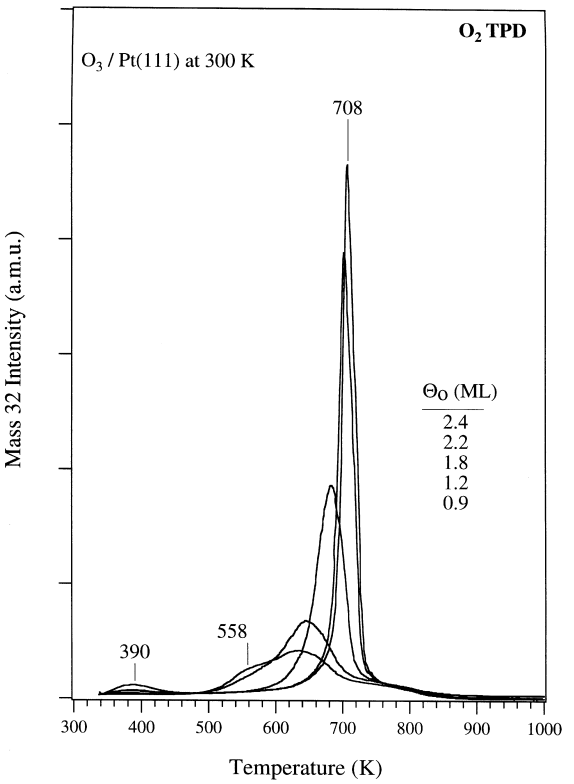

Fig. 2. O_2 TPD curves following O_3 exposures of 1 to 20 L on Pt(111) at 300 K.

temperatures as the oxygen coverage increased, and occurred at 742 K for $\Theta_O = 0.19$ ML. With increased oxygen coverage, an additional desorption peak appeared and O_2 desorbed at lower temperatures between 678 and 663 K. At $\Theta_O \geq 0.54$ ML, an additional structure occurred at temperatures of 634 and 558 K. For $\Theta_O = 0.73$ ML, the O_2 desorption profile was similar to those seen previously following NO_2 exposures on Pt(111) at 400 K with $\Theta_O = 0.75$ ML [12].

The TPD spectra of O_2 desorption for $\Theta_O = 0.95$–2.4 ML are shown in Fig. 2. With increasing amounts of oxygen greater than $\Theta_O = 0.95$ ML, the peak at 634 K increased in intensity, sharpened, and shifted to a higher temperature. A very sharp peak (23 K wide) at 708 K was finally observed at $\Theta_O = 2.4$ ML. Also, oxygen evolution was observed at very low temperatures in a peak near 390 K at these high coverages. The leading edges (low-temperature parts) of the

desorption curves for $\Theta_O > 0.95$ ML crossed through, "undercutting" those of the lower coverage TPD curves. This interesting behavior was also seen previously for large oxygen concentrations on Pd(111) [13]. Masel [29] and Campbell [30] discussed such behavior in TPD as arising from surface tension effects for finite-sized islands (PtO_x in our case, vide supra).

The O_2 desorption activation energy, E_d, is an important parameter to elucidate, for example it is needed for calculating the Pt–O bond strength and the oxygen residence time. In order to estimate values of E_d, we used the method from Ref. [31], which is derived from the Polanyi–Wigner equation and provides E_d and a determination of the reaction order, n. In the region of the onset of desorption (at low temperatures), this method gives the same results as the leading edge method [32,33]. The slope of a plot of $\ln(-d\Theta/dt) - n \ln\Theta$ versus $1/T$ gives a value for E_d, and for some cases, this plot can also be used to determine n. For example, several of these curves are shown in Fig. 3. Plots for $\Theta_O < 0.32$ ML are most consistent with $n = 2$. The desorption activation energy determined from the slopes of these lines varies from 45 to 32 kcal mol^{-1} for $\Theta_O = 0.03$–0.32 ML. For $0.32 < \Theta_O < 0.95$ ML, the rate approaches a more linear dependence on Θ_O, i.e. $n < 2$, and two linear regions are observed at temperatures below T_p. Using the leading edges of the desorption traces, because this region is least affected by coverage and temperature-dependent effects, the slopes at a low temperature yield values of E_d that decrease from 32 kcal mol^{-1} at $\Theta_O = 0.32$ ML to 26 kcal mol^{-1} at $\Theta_O = 0.95$ ML (Fig. 3c). Our values of E_d for $\Theta_O < 0.75$ ML show the same trend with coverage, and the values agree within ± 5 kcal mol^{-1} from those reported in Ref. [12].

For $\Theta_O > 0.95$ ML, plots such as those shown in Fig. 3d have no linear region over any appreciable temperature range for $n = 0$–2. It could be that one or both of the pre-exponential term and desorption activation energy are coverage-dependent, and the concept of a reaction order is lost [34], or the Polanyi–Wigner equation is not applicable. However, we can still estimate E_d by considering these plots. Using the leading edges, E_d varies from 26 to 23 kcal mol^{-1} for $\Theta_O = 0.95$ to 2.4 ML, respectively. This desorption energy characterizes weakly bound oxygen on the surface. Most of the oxygen present on the surface is more strongly bound than this, and desorbs in a peak that varies from 630 to 708 K. However, we cannot obtain E_d from plots like those in Fig. 3d for the oxygen that desorbs near T_p. The only estimate we can make is to use Redhead analysis [35], assuming first- or half-order desorption kinetics and a normal prefactor, and the measured value of T_p to determine that E_d varies from 35 to 42 kcal mol^{-1} for a large amount of oxygen existing at $\Theta_O = 0.95$ to 2.4 ML.

In summary, E_d initially decreases as the coverage increases until $\Theta_O \sim 1$ ML because of lateral repulsive interactions. A minimum in the value of E_d occurs because E_d increases for oxygen concentrations exceeding about one monolayer. We propose that this minimum in E_d corresponds to a phase change of chemisorbed oxygen adatoms as nucleation of platinum oxide occurs. The increase in E_d at larger concentrations arises from either attractive lateral interactions or increasing sizes of the PtO_x particles formed.

Oxygen uptake curves for O_3 and O_2 exposures on Pt(111) at 300 K are shown in Fig. 4. These were constructed by using the subsequent O_2 TPD peak areas. Both gases were dosed under identical conditions using the same microcapillary array doser. Exposures reported here are not corrected for doser enhancement or ion gauge sensitivity. Also, the purity of the dosed O_3 actually incident on the surface was not ascertained. Exposures equal to or greater than 6 L O_2 on Pt(111) saturate the surface with oxygen adatoms, which we define to be a coverage of $\Theta_O = 0.25$ ML [3,9]. Oxygen uptake from ozone saturates at $\Theta_O = 2.4$ ML and could be produced by an exposure of 20 L.

The initial sticking coefficient (S_0) of ozone on Pt(111) at 300 K was estimated by a comparison of O_2 and O_3 uptake curves at small exposures (below 0.5 L), as shown in the inset of Fig. 4. The slopes of the fitted lines were used to determine that $S_0(O_3)$ has a value of $S \geq 0.24$ since $S_0(O_2) = 0.05$ on Pt(111) at 300 K [6,36,37]. This gives a lower limit on the O_3 sticking coefficient because of the presence of impurities (mostly O_2 and H_2O) with lower sticking probabilities that

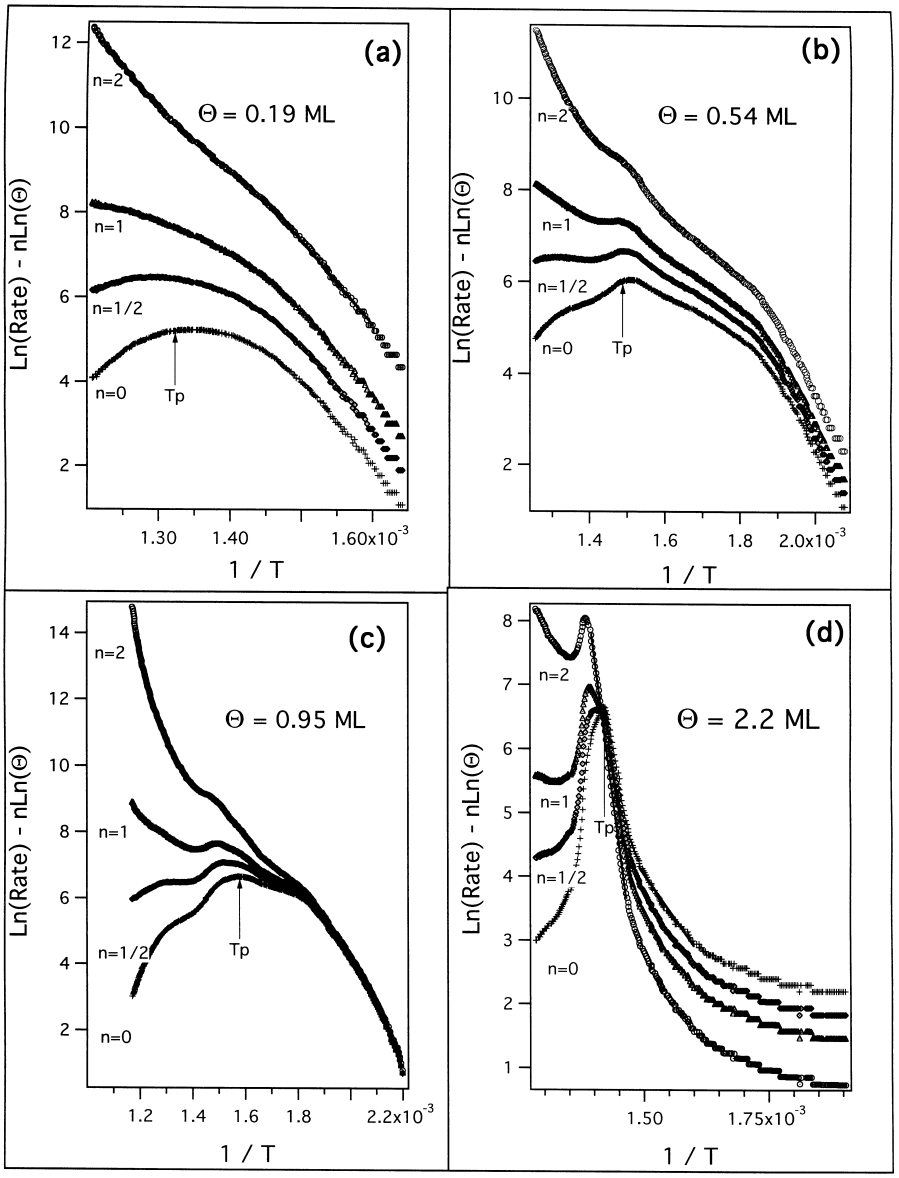

Fig. 3. Arrhenius plots of the O_2 TPD curves for oxygen concentrations of (a) 0.19, (b) 0.54, (c) 0.95 and (d) 2.2 ML using the method of Parker et al. [31]. For the several curves shown here, a straight line was obtained when $n=2$ for $\Theta_O=0.19$ ML, but for the other coverages shown, no choice of $n=0$–2 gave linear plots over the entire desorption range.

are generated in the gas handling lines prior to O_3 dosing.

AES was also used to follow oxygen uptake from O_3 exposures on Pt(111) at 300 K. Fig. 5 shows the changes in the AES signals versus the oxygen coverage determined by O_2 TPD peak areas. The intensity of the O(507 eV) signal increases linearly up to a saturation oxygen concentration of 2.4 ML. Concomitantly, the Pt(237 eV) signal decreases linearly over the same oxygen coverage region. This behavior indicates that oxidation at 300 K does not lead to oxygen

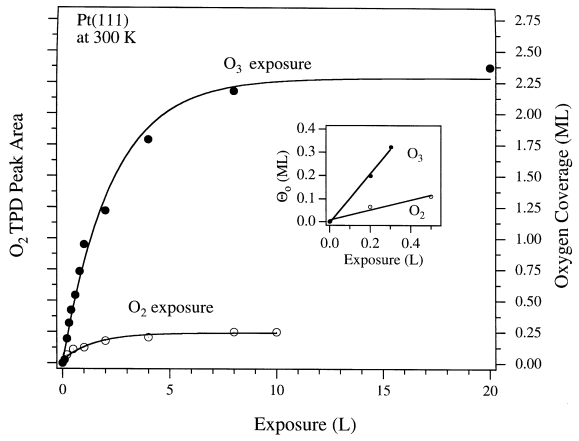

Fig. 4. Oxygen uptake curves comparing the efficiency of O_3 and O_2 exposures on Pt(111) at 300 K. The inset shows details for oxygen accumulation from O_3 and O_2 at low exposures.

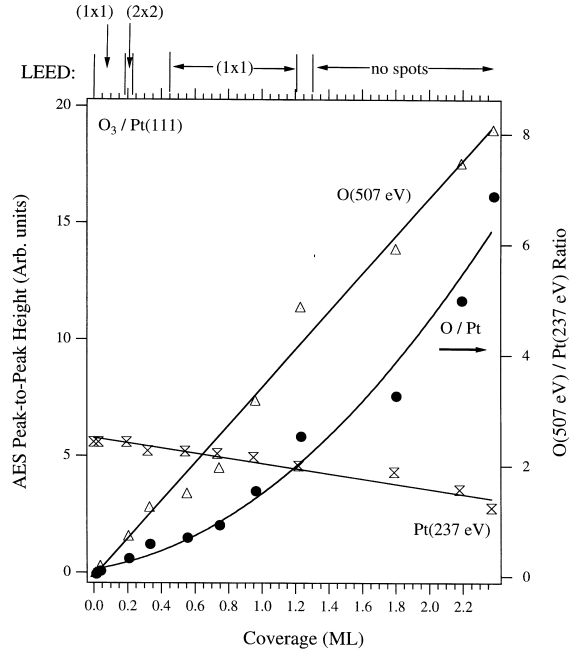

Fig. 5. AES intensities and the O (507)/Pt (237) AES ratio are shown as a function of oxygen coverage, Θ_O, as determined by O_2 TPD peak areas. The result of concurrent LEED measurements are shown along the top bar.

dissolving deep into the bulk. The top of Fig. 5 provides a characterization of the surface order by LEED during oxygen uptake. A sharp (2×2) LEED pattern was observed after O_3 exposures that produced $\Theta_O=0.19$–0.32 ML. O_2 exposures on Pt(111) at 300 K also gave a sharp (2×2) LEED pattern at $\Theta_O=0.25$ ML. For $\Theta_O<0.19$ ML and for $0.32<\Theta_O<1.2$ ML, a (1×1) pattern was exhibited. Following O_3 exposures forming $\Theta_O>1.0$ ML, the (1×1) LEED pattern disappears. We ascribe this disordering of the surface Pt atoms to incorporated subsurface oxygen or the nucleation of platinum oxide particles (vide infra).

Fig. 6 shows that the Pt and O AES peaks shift during oxygen uptake. The kinetic energy for the Pt(NNO) transition shifts gradually lower by 0.8 eV with increasing oxygen coverage, implying that Pt oxidation is taking place at room temperature at high oxygen coverages. Also, the O (KVV) peak shifts up by 1.6 eV, and the Auger lineshape changes, consistent with a change in the chemical

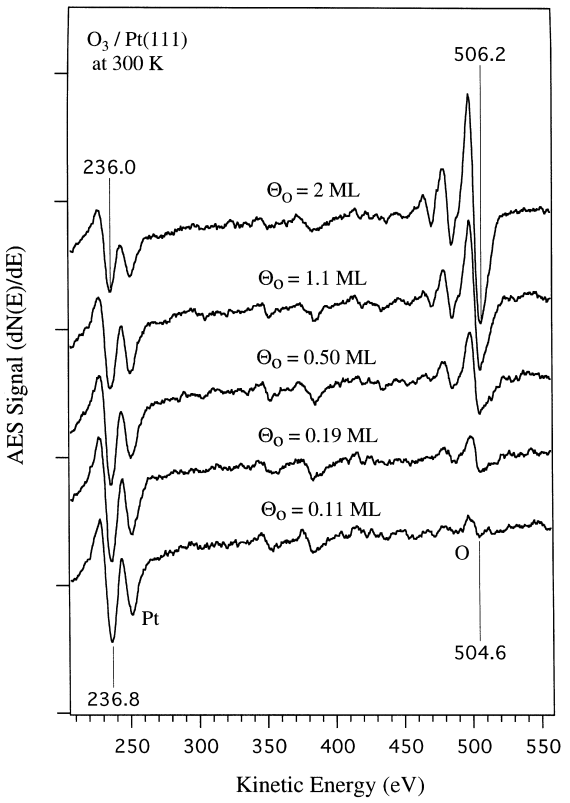

Fig. 6. AES spectra for increasing O_3 exposures on Pt(111) at 300 K. Shifts of the Pt and O AES peaks indicate changes in chemical state due to oxidation.

state of oxygen at high coverages. The O (KVV) lineshape from an oxidized surface ($\Theta_O = 1.8$ ML) is shown more clearly in Fig. 7. The main features of the $dN(E)/dE$ curves, including maxima, minima, zero-level crossings, and inflection points are marked from (1) to (15). In this spectrum, $D_1 = E(9)–E(12)$, $D_2 = E(7) - E(12)$, $D_3 = E(2)–E(12)$ and $D_4 = E(14)–E(12)$ were calculated to be -12.9, -19.0, -33.1 and 10.9 eV, respectively. These values are close to those reported for many bulk oxides [38]. In addition, the presence of feature (5) assigned to the bulk plasmon on the ^{1}D transition is also characteristic of oxides [38]. For oxygen coverages below 1.2 ML, this latter feature was not seen, and the values of D_1–D_4 were different.

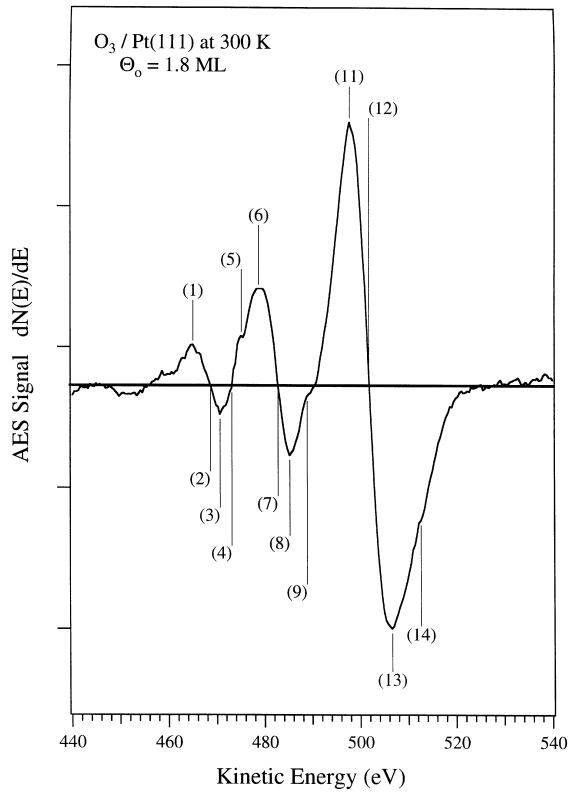

Fig. 7. O (KVV) lineshape for $\Theta_O = 1.8$ ML on Pt(111). The features denoted by labels correspond to characteristics in the lineshape used to derive chemical state information, specifically the presence of oxidic oxygen.

4. Discussion

Ozone (O_3) is a strong oxidant that can be used to reach high "effective" O_2 pressures under UHV conditions and oxidize noble metal surfaces. Adsorption of ozone on Pt(111) at 300 K efficiently leads to an oxygen-covered surface, with a sticking coefficient, S, at zero coverage of $S_0 \geq 0.24$ and high values of S for $\Theta_O > 1$ ML. We propose that two chemical states of oxygen can readily be formed, a chemisorbed oxygen adlayer for $\Theta_O \leq 1$ ML and PtO_x particles at high concentrations, which can reach up to $\Theta_O = 2.4$ ML. Previously, Parker et al. [12] utilized NO_2 exposures on Pt(111) at 400 K to produce $\Theta_O = 0.75$ ML. Under these conditions, no molecular chemisorbed oxygen was formed, no "oxidic" oxygen was observed, and only chemisorbed oxygen was formed. The presence of multiple peaks in the resultant O_2 desorption in TPD was interpreted as arising from a combination of decreases in the Pt–O bond strength and increases in the barrier to dissociative chemisorption of O_2 on Pt(111).

The results herein can be compared to analogous studies on Pd(111) [39]. Pd is much more easily oxidized than Pt, and extensive oxidation can be achieved in UHV by exposing NO_2 onto the Pd(111) surface at 530 K [39]. Chemisorbed oxygen is formed on Pd(111) at low NO_2 exposures, but an oxide forms at or near the surface at high oxygen concentrations ($\Theta_O > 1$ ML). The concentration of oxygen on Pd(111) reported in Ref. [39] as $\Theta_O = 1.4$ ML should be corrected to $\Theta_O = 1$ ML due to an error in Ref. [39]. When oxygen is dosed on Pd(111) at 110 K, a saturation coverage of $\Theta_O = 0.17$ ML is obtained instead of $\Theta_O = 0.25$ ML. The O_2 TPD spectra that we observed over the entire oxygen coverage range on Pt(111) was qualitatively like that previously reported on Pd(111). The sharp O_2 TPD peak (30 K FWHM) at 715 K was given as characteristic of the decomposition of PdO_x upon heating in UHV [39]. This peak temperature was similar to that for the decomposition of PdO in UHV between 720 and 820 K reported by Peuckert [22] and also to the decomposition of PtO_x that we observed at 708 K.

Rh is also more easily oxidized than Pt, and

oxidation of Rh(111) using NO_2, NO, and O_2 in UHV [40–43] and high pressures of O_2 [44] has been investigated. Undercutting of the O_2 TPD peaks with increasing oxygen coverage and narrow O_2 TPD peaks for decomposition of Rh_2O_3 [44] was observed.

Recently, we have observed similar O_2 TPD curves after exposing ozone to the Pt(100) surface at 300 K [25]. TPD for $\Theta_O < 0.85$ ML showed multiple O_2 desorption peaks at 567, 632, 664 and 687 K, and for higher coverages showed a sharp peak at 566 K that shifted to higher temperatures (660 K) with increasing concentrations. The sharp O_2 desorption peaks were shown to arise from the formation of PtO_x by utilizing XPS. Interestingly, the decomposition temperature of PtO_x from the Pt(111) surface (708 K) is higher than that on the Pt(100) surface (660 K). This difference could be due to either a thermodynamic or a kinetic effect, and this is discussed elsewhere.

Ozone is a much stronger oxidizing agent than NO_2, and is capable of oxidizing one of the noblest of all metals: Au [24]. Exposures of ozone on the Au(111) surface at 300 K produced chemisorbed oxygen with $\Theta_O = 1.2$ ML. Oxygen adsorption at this high coverage disorders the Au(111) surface probably due to incorporation of oxygen into the surface layer. On Au(111), O_2 TPD curves could be described by first-order desorption kinetics, and no "undercutting" of the O_2 peak leading edges was observed as in the cases of Pt(111), Pd(111), and Rh(111). The apparent first-order O_2 desorption kinetics on Au(111) was explained by the presence of a rate-limiting step other than recombination of two O adatoms, which we attributed to the conversion of an oxidic AuO_x species to chemisorbed oxygen.

The type of lateral interactions undoubtedly present at such high coverages of oxygen adatoms on metal surfaces and under conditions where oxide particles are formed causes strong effects in the O_2 thermal desorption profiles. Masel [29] showed with simulation studies that multiple peaks can arise in TPD spectra when repulsive interactions between nearest-neighbors occur. Also, attractive interactions can lead to the type of undercutting in the leading edges of peaks in TPD spectra that we observed because of clustering of the adsorbates into small particles which stabilize them on the surface. As a result, the desorption temperature increases, and the desorption rate decreases at a given temperature, as the coverage increases. Such narrow TPD profiles and undercutting behavior have also been referred to as "surface explosions" by many authors. In our work, the transition from repulsive to attractive lateral interactions is accompanied by a profound change in the TPD spectra with oxygen coverage at about $\Theta_O = 1.2$ ML. This coverage evidently corresponds to a change in the competition between oxygen diffusion into the subsurface region, O_2 desorption, and nucleation of PtO_x particles at or near the surface.

If small nanoclusters of PtO_x particles are indeed formed, one might expect that changes in cluster size with extent of oxidation would affect the thermal stability of these clusters probed by O_2 TPD. The sizes of platinum oxides particles might even be crudely estimated based on the well-known influence of particle size on vapor pressure in liquid–vapor equilibria. The ratio of vapor pressure for small spherical particles of radius r compared to the bulk material, P_r/P_{bulk}, is given by the Kelvin equation [45]:

$$P_r/P_{bulk} = \exp[(2\gamma_{v/m}M)/(\rho r R T)], \quad (1)$$

where R is the gas constant, M is the molecular weight, ρ is the density of the condensed phase, T is the temperature and $\gamma_{v/m}$ is the surface tension of the particle. In order to make a rough estimate, assume that the O_2 TPD curve for an oxygen coverage of 2.4 ML (Fig. 2) represents desorption from large, bulk-like oxide particles. The vapor pressure ratio (P_r/P_{bulk}) for $\Theta_O = 1.2$ ML taken at 644 K is equal to 4.06. Assuming that PtO_2 is formed with a density of 10.2 g cm^{-3} [46] and a molecular weight of 227.08 g [46], and that the surface tension is 600 ergs cm^{-2}, which is that of Ag_2O [47] (since that of PtO_2 is not available), Eq. (1) gives a radius for the oxide particles of approximately 35 Å for $\Theta_O = 1.2$ ML. We can check whether this estimate is reasonable by considering the desorption energetics. Assuming that we have the same prefactor for desorption, $E_{des,r} - E_{des,bulk}$ is equal to $-RT\ln(P_r/P_{bulk})$ or $-(2\gamma_{v/m}M)/(\rho r)$. This gives $E_{des,r} - E_{des,bulk} =$

-2 kcal mol^{-1}, which can be compared to -3 kcal mol^{-1} calculated by the leading edge analysis or -2 kcal mol^{-1} calculated by Redhead analysis. Hence, the particle size of 35 Å for $\Theta_O = 1.2$ ML may be a reasonable estimate, even though there are limitations to the application of the Kelvin equation for small particles [48], and bonding interactions between the PtO_x and Pt metal atoms modify surface free energies.

In summary, we propose the following model for describing the chemical nature of the oxygen formed by O_3 exposure on Pt(111) at 300 K. For $\Theta_O < 1$ ML, oxygen adatoms are formed. Complex, multiple-peak O_2 TPD spectra result because of strong lateral repulsive interactions within this oxygen adlayer. "Oxidic" oxygen is formed when the oxygen coverage reaches ~ 1.2 ML, and PtO_x particles grow in size at or near the surface until an oxygen concentration of $\Theta_O = 2.4$ ML is reached. At this point, the O_3 dissociative adsorption rate constant decreases to a negligible value.

5. Conclusions

High concentrations of surface oxygen can be readily achieved on the Pt(111) surface at 300 K in UHV via exposures of ozone (O_3). Oxygen coverages as high as 2.4 ML were reached forming a disordered oxidic film at 300 K. For $\Theta_O \leq 1$ ML, chemisorbed oxygen adatoms are formed. Higher oxygen concentrations nucleate small particles of PtO_x at or near the surface. O_2 thermal desorption for coverages of $\Theta_O < 1$ ML shifts strongly to a lower temperature, with TPD peaks decreasing from 814 to 558 K with increasing Θ_O because of repulsive lateral interactions that weaken the Pt–O bond. The activation energy of O_2 desorption, E_d, decreases from 45 kcal mol^{-1} at $\Theta_O = 0.2$ ML to roughly 26 kcal mol^{-1} at $\Theta_O = 1$ ML. For $\Theta_O = 1.2$–2.4 ML, the O_2 desorption temperature shifts to a higher temperature (from 644 to 708 K) as the oxygen concentration increases because of strong attractive lateral interactions responsible for growth of PtO_x particles. The value of E_d involving PtO_x decomposition increases with coverage from ~ 21 kcal mol^{-1} at $\Theta_O = 1.2$ ML to ~ 23 kcal mol^{-1} at $\Theta_O = 2.4$ ML.

Acknowledgements

This work was supported by the Division of Chemical Sciences, Office of Basic Energy Sciences, US Department of Energy.

References

[1] T. Engel, G. Ertl, in: D.A. King, D.P. Woodruff (Eds.), The Chemical Physics of Solid Surfaces and Heterogeneous Catalysis, Vol. 4, Elsevier, Amsterdam, 1982, Ch. 3.
[2] P.R. Norton, in: D.A. King, D.P. Woodruff (Eds.), The Chemical Physics of Solid Surfaces and Heterogeneous Catalysis, Vol. 4, Elsevier, Amsterdam, 1982, Ch. 2.
[3] J.L. Gland, Surf. Sci. 93 (1980) 487.
[4] J.L. Gland, B.A. Sexton, G.B. Fisher, Surf. Sci. 95 (1980) 587.
[5] S.K. Shi, J.M. White, R.L. Hance, J. Phys. Chem. 84 (1980) 2441.
[6] C.T. Campbell, G. Ertl, H. Kuipers, J. Segner, Surf. Sci. 107 (1981) 220.
[7] H. Steininger, S. Lehwald, H. Ibach, Surf. Sci. 123 (1982) 1.
[8] P.R. Norton, J.A. Davies, T.E. Jackman, Surf. Sci. 122 (1982) L593.
[9] D. Neuhaus, F. Joo, B. Feuerbacher, Phys. Rev. Lett. 58 (1987) 694.
[10] K. Mortensen, C. Klink, F. Jensen, F. Besenbacher, I. Stensgaard, Surf. Sci. 220 (1989) L701.
[11] M.E. Bartram, R.G. Windham, B.E. Koel, Surf. Sci. 184 (1987) 57.
[12] D.H. Parker, M.E. Bartram, B.E. Koel, Surf. Sci. 217 (1989) 489.
[13] G. Tremiliosi-Filho, G. Jerkiewicz, B.E. Conway, Langmuir 8 (1992) 658 and references therein.
[14] B.E. Conway, G. Jerkiewicz, J. Electroanalyt. Chem. 339 (1992) 123.
[15] R.J. Berry, Surf. Sci. 76 (1978) 415.
[16] C.G. Vayenas, J.N. Michaels, Surf. Sci. 120 (1982) L405.
[17] H. Neff, S. Henkel, E. Hartmannsgruber, E. Steinbeiss, W. Michalke, K. Steenbeck, H.G. Schmidt, J. Appl. Phys. 79 (1996) 7672.
[18] W.D. Westwood, C.D. Bennewitz, J. Appl. Phys. 45 (1974) 2313.
[19] M. Salmeron, L. Brewer, G.A. Somorjai, Surf. Sci. 112 (1981) 207.
[20] T. Wang, A. Vazquez, A. Kato, L.D. Schmidt, J. Catal. 78 (1982) 306.
[21] M. Peuckert, H.P. Bonzel, Surf. Sci. 145 (1984) 239.

[22] M. Peuckert, J. Phys. Chem. 89 (1985) 2481.
[23] S.W. Benson, Thermochemical Kinetics, Wiley, New York, 1996.
[24] N.A. Saliba, D.H. Parker, B.E. Koel, Surf. Sci 410 (1998) 270.
[25] D.E. Beck, N.A. Saliba, C. Baur, B.E. Koel, in preparation.
[26] N.A. Saliba, Y.L. Tsai, B.E. Koel, J. Phys. Chem. submitted.
[27] N.A. Saliba, D.E. Beck, C. Baur, B.E. Koel, in preparation.
[28] R.G. Windham, M.E. Bartram, B.E. Koel, J. Phys. Chem. 92 (1988) 2862.
[29] R.I. Masel, Principles of Adsorption and Reaction on Solid Surfaces, 1st ed., Wiley, New York, 1996, p. 536.
[30] C.T. Campbell, Surf. Sci. Rep. 27 (1997) 1.
[31] D.H. Parker, M.E. Jones, B.E. Koel, Surf. Sci. 233 (1990) 65.
[32] E. Habenschaden, J. Kuppers, Surf. Sci. 138 (1984) L147.
[33] J.B. Miller, H.R. Siddiqui, S.M. Gates, J.N. Russell, J.T. Yates Jr., J.C. Tully, J.M. Cardillo, J. Chem. Phys. 87 (1987) 6725.
[34] D.A. King, in: R. Vanselow (Ed.), Chemistry and Physics of Solid Surfaces, Vol. II, CRC Press, Boca Raton, FL, 1979, p. 87.
[35] P.A. Redhead, Vacuum 12 (1962) 203.
[36] F. Eisert, A.P. Elg, A. Rosen, Appl. Phys. A 60 (1995) 209.
[37] A.P. Elg, F. Eisert, A. Rosen, Surf. Sci. 382 (1997) 57.
[38] P. Legare, G. Maire, B. Carriere, J.P. Deville, Surf. Sci. 68 (1977) 348.
[39] B.A. Banse, B.E. Koel, Surf. Sci. 232 (1990) 275.
[40] X. Guo, L. Hanley, J.T. Yates Jr., J. Chem. Phys. 90 (1989) 5200.
[41] K.D. Gibson, J.I. Colonell, S.J. Sibener, Surf. Sci. 343 (1995) L1151.
[42] K.A. Peterlinz, S.J. Sibener, Surf. Sci. 344 (1995) L1239.
[43] K.A. Peterlinz, S.J. Sibener, J. Phys. Chem. 99 (1995) 2817.
[44] A.D. Logan, A.K. Datye, J.E. Houston, Surf. Sci. 245 (1991) 280.
[45] A.W. Adamson, A.P. Gast, Physical Chemistry of Surfaces, 6th ed., Wiley, New York, 1997, p. 54.
[46] D.R. Lide (Ed.), CRC Handbook of Chemistry and Physics, 73rd ed., CRC Press, Boca Raton, FL, 1992–1993.
[47] S.H. Overburry, P.A. Bertrand, G.A. Somorjai, Chem. Rev. 75 (1975) 547.
[48] L.S. Fisher, J.N. Israelachvili, J. Colloid Interf. Sci. 80 (1981) 528.